

Chemical Science

rsc.li/chemical-science



ISSN 2041-6539



ROYAL SOCIETY
OF CHEMISTRY

Celebrating
IYPT 2019

EDGE ARTICLE

Harunobu Mitsunuma, Motomu Kanai *et al.*
Catalytic asymmetric allylation of aldehydes with alkenes through allylic C(sp³)-H functionalization mediated by organophotoredox and chiral chromium hybrid catalysis

Cite this: *Chem. Sci.*, 2019, 10, 3459

All publication charges for this article have been paid for by the Royal Society of Chemistry

Catalytic asymmetric allylation of aldehydes with alkenes through allylic C(sp³)-H functionalization mediated by organophotoredox and chiral chromium hybrid catalysis†

Harunobu Mitsunuma,^a Shun Tanabe,^a Hiromu Fuse,^a Kei Ohkubo^b and Motomu Kanai^a

We describe a hybrid system that realizes cooperativity between an organophotoredox acridinium catalyst and a chiral chromium complex catalyst, thereby enabling unprecedented exploitation of unactivated hydrocarbon alkenes as precursors to chiral allylchromium nucleophiles for asymmetric allylation of aldehydes. The reaction proceeds under visible light irradiation at room temperature, affording the corresponding homoallylic alcohols with a diastereomeric ratio >20/1 and up to 99% ee. The addition of Mg(ClO₄)₂ markedly enhanced both the reactivity and enantioselectivity.

Received 19th December 2018
Accepted 16th January 2019

DOI: 10.1039/c8sc05677c

rsc.li/chemical-science

Introduction

Catalytic asymmetric C(sp³)-H bond functionalization is an emerging synthetic method affording direct access to useful chiral building blocks from stable organic molecules.¹ For example, catalytic asymmetric allylation of aldehydes using unactivated alkenes as pronucleophiles produces enantiomerically-enriched homoallylic alcohols, which act as versatile synthetic intermediates for numerous functional molecules, including various drug leads.² The catalytic asymmetric carbonyl ene reaction is a representative example (Fig. 1(a)).³ The electrophile scope of catalytic asymmetric carbonyl ene reactions, however, is limited to highly reactive aldehydes or ketones, such as glyoxylic esters, formaldehyde, fluoral, or ketoesters. In an effort to expand the substrate scope, we envisioned that a reaction mechanism dissected by chiral nucleophilic allylmetal species, which are generated from alkenes *via in situ* allylic C(sp³)-H bond activation, would be feasible.⁴ Some previous examples related to this strategy are reported. Gong presented a one-pot procedure for asymmetric nucleophilic allylation of an aldehyde with an alkene involving palladium-catalyzed allylic C(sp³)-H borylation of the alkene to generate an allylboronate and chiral phosphoric acid-catalyzed asymmetric allylation of the aldehyde with the thus-generated allylboronate (Fig. 1(b)).⁵ Mita and Sato reported a cobalt-catalyzed enantioselective allylation

between acetone and an allylarene *via* nucleophilic chiral allyl-cobalt(i) species generated through oxidative addition of an allylic C(sp³)-H bond to a low valent cobalt complex (Fig. 1(c)).⁶ During our study, Glorius' group reported an asymmetric allylation between an aldehyde and an allylamine mediated by combining an iridium photoredox catalyst and a chiral chromium catalyst (Fig. 1(d)).⁷ Considering the attractive feature of this reaction to generate versatile chiral homoallylic alcohols in a single operation from aldehydes and alkenes, further investigation of this reaction type are highly desirable.^{8,9}

Photocatalyzed C(sp³)-H bond activation followed by oxidative interception of the resulting carbon-centered radical by a metal complex catalyst is a groundbreaking concept for generating organometallic intermediates from substrates traditionally considered inert.¹⁰⁻¹³ Application of organometallic intermediates generated by this method, however, has mainly been limited to cross-coupling reactions. Extension of the chemistry to facilitate the addition of these nucleophiles to polar moieties, such as carbonyl groups, has yet to be explored, except for the recent example by Glorius using electron-rich aromatic- or amine-substituted alkenes.⁷ Herein we report an asymmetric hybrid catalyst system comprising an organophotoredox catalyst and a chiral chromium complex catalyst, which enables asymmetric allylation of aldehydes by nucleophilic chiral allylchromium species generated *in situ* from hydrocarbon feedstock alkenes by C(sp³)-H bond activation (Fig. 1(d)).

Results and discussion

Optimization of reaction conditions

Our mechanistic rationale for this transformation is illustrated in Fig. 2. Based on an earlier report by the Wu laboratory,¹⁴ allyl

^aGraduate School of Pharmaceutical Sciences, The University of Tokyo, 7-3-1 Bunkyo-ku, Tokyo 113-0033, Japan. E-mail: h-mitsunuma@mol.f.u-tokyo.ac.jp; kanai@mol.f.u-tokyo.ac.jp

^bInstitute for Advanced Co-Creation Studies, Open and Transdisciplinary Research Initiatives, Osaka University, Osaka 565-0871, Japan

† Electronic supplementary information (ESI) available. See DOI: 10.1039/c8sc05677c





Fig. 1 Methods for catalytic asymmetric allylation of carbonyl compounds through C(sp³)-H functionalization of unactivated alkenes as pronucleophiles. (a) Chiral Lewis acid or Brønsted acid-catalyzed carbonyl ene reactions.³ (b) One-pot, stepwise generation of allylboration followed by chiral Brønsted acid-catalyzed allylboration.⁵ (c) Through chiral allylcobalt species.⁶ (d) Through chiral allylchromium species by Glorius⁷ and our group (this work).

radical **4** should be accessible from alkene **1a** via electron-transfer oxidation of the π -bond by a photoexcited electron-donor substituted acridinium catalyst (D⁺-Acr⁺; D = 2,6-xylyl or mesityl) to generate radical cation **3**, followed by deprotonation. A reduced form of the chiral chromium(II) catalyst **5** would then intercept the thus-formed allyl radical **4** to give chiral allylchromium(III) complex **6**. We anticipated that this species would react with aldehydes **2** via a six-membered chair transition state to produce enantiomerically-enriched chromium alkoxide **7** in a *syn*-selective manner. Protonolysis of **7**



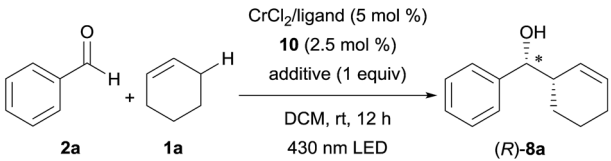
Fig. 2 Proposed catalytic cycle.

would then afford the target homoallylic alcohol **8** and an oxidized chromium(III) complex **9**. Finally, electron-transfer reduction of **9** by the reduced form of the photocatalyst (D-Acr⁺) would regenerate **5** and the oxidized form of the photocatalyst (D-Acr⁺), thus closing the catalytic cycle.¹⁵

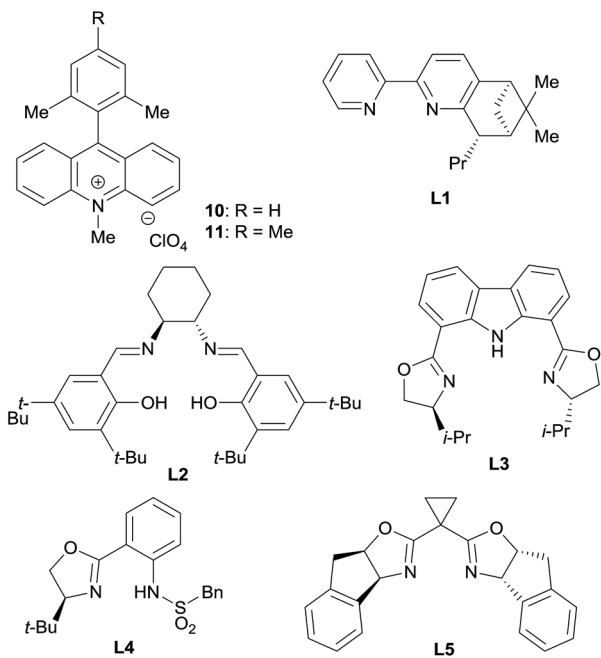
Based on this hypothesis, we began optimizing the reaction conditions using benzaldehyde (**2a**) and cyclohexene (**1a**: 20 equiv.) as model substrates, and a combination of 5 mol% CrCl₂ and 2.5 mol% acridinium photoredox catalysts (2,6-Xyl-Acr⁺·ClO₄⁻; **10**),¹⁶ under 430 nm visible light irradiation at room temperature (Table 1). As expected, the desired reaction did not proceed at all in the absence of the chromium complex (entry 1). In the presence of CrCl₂, however, **8a** was obtained in 36% yield with an excellent diastereomeric ratio (dr) of >20/1 (entry 2). Encouraged by this finding, we then screened various chiral ligands for the chromium catalysts that were previously shown to be effective for asymmetric Nozaki-Hiyama-Kishi reactions (entries 3–6).¹⁷ The chiral catalysts strongly retarded the reaction, however, with only **L1** (ref. 18) affording **8a** with diminished yield (12%) and low enantioselectivity (20% ee). Through extensive screening of other chiral ligands, we identified an indane-BOX ligand (**L5**)¹⁹ that effectively induced good enantioselectivity (74% ee), although the yield of **8a** remained unsatisfactory (8%, entry 7).

We supposed that the low reactivity was due to the high oxidation potential of **1a**. Due to the small oxidation potential difference between substrate **1a** and photoredox catalyst **10** (see ESI†), only low concentration of cation radical **3** were generated. To improve the reactivity, we investigated the effects of salt additives to stabilize cation radical **3**, which would accelerate the overall reaction rate.²⁰ Screening of several electrolytes revealed that adding LiBF₄ dramatically enhanced the reactivity; **8a** was obtained in 40% yield with 63% ee (entry 8). Moreover, the use of LiClO₄ increased the enantioselectivity up to 99% (entry 9). Further exploration of alkali and alkali-earth metal



Table 1 Optimization of the reaction conditions^a


Entry	Ligand	Additive	Yield (%)	dr	ee (%)
1 ^b	None	None	0	n.d.	n.d.
2	None	None	36	>20/1	n.d.
3	L1	None	12	>20/1	20
4 ^c	L2	None	0	n.d.	n.d.
5 ^d	L3	None	0	n.d.	n.d.
6 ^d	L4	None	0	n.d.	n.d.
7	L5	None	8	>20/1	74
8	L5	LiBF ₄	40	>20/1	63
9	L5	LiClO ₄	44	>20/1	99
10	L5	NaClO ₄	14	>20/1	99
11	L5	Ca(ClO ₄) ₂ · xH ₂ O	8	>20/1	98
12	L5	Mg(ClO ₄) ₂	68	>20/1	99
13 ^e	L5	Mg(ClO ₄) ₂	63	>20/1	99



^a General reaction conditions: **2a** (0.25 mmol), **1a** (5.0 mmol), CrCl₂ (0.0125 mmol), ligand (0.0125 mmol), **10** (0.00625 mmol), and additive (0.25 mmol) were reacted in dichloromethane (DCM; 2.5 mL) at room temperature under 430 nm LED irradiation for 12 h. Yield and diastereomeric ratio were determined by ¹H NMR analysis of the crude mixture using 1,1,2,2-tetrachloroethane as an internal standard. The enantioselectivity of **8a** was determined by chiral stationary HPLC analysis after isolation. n.d. = not determined. ^b Without CrCl₂. ^c 10 mol% Et₃N was added. ^d 5 mol% Et₃N was added. ^e Mes-Acr⁺ · ClO₄⁻ **11** was used as a photocatalyst.

perchlorates (entries 10–12) identified Mg(ClO₄)₂ as the optimal additive; **8a** was obtained in 68% yield with >20/1 dr and 99% ee (entry 12). Additionally, the use of phthalate instead of a xylyl group, did not negatively affect these results (entry 13). It is noteworthy that compared to

traditional catalytic asymmetric carbonyl allylations,² except for the Krische's method,^{2i,p} this reaction can bypass the pre-activation step of the nucleophile using stoichiometric metal species.

Substrate scope

Under these optimized conditions, we next evaluated the substrate scope (Table 2). The reaction of cyclohexene (**1a**) with substituted benzaldehydes afforded products **8a–8g** with almost complete diastereo- and enantioselectivity (up to >20/1 dr, 99% ee). The reaction well tolerated aryl halide moieties (**8b–8d**), and proceeded chemoselectively at the aldehyde functional group in the presence of a ketone (**8e**) or an ester (**8f**) functional group. The method was also easily extended to other cyclic alkenes, with both cyclopentene (**1b**) and cycloheptene (**1c**) reacting with excellent stereoselectivity (**8h–8k**).

Linear alkenes were also competent substrates. Tetrasubstituted alkene **1d** reacted with various aldehydes, including *ortho*-, *meta*-, and *para*-substituted benzaldehydes, an electron-rich benzaldehyde, and a heteroaromatic aldehyde, affording the corresponding products **8l–8q** (containing an allylic quaternary carbon) with excellent enantioselectivity. The loading of alkene **1d** could be reduced to 2 equiv., likely due to the lower oxidation potential of **1d** relative to **1a–1c**. For less reactive aldehydes such as *o*-tolualdehyde and *p*-methoxy benzaldehyde, the chiral chromium alkoxide complex generated from CrCl₃ · 3THF and NaOt-Bu²¹ exhibited higher catalytic activity than the CrCl₂-derived species (**8m** and **8p**). We postulate that this is as a result of allylchromium species **6** bearing alkoxide ligands (X = OR) with higher nucleophilicity than those bearing electron-withdrawing chloride ligands (X = Cl).^{22,23} The reaction of aliphatic aldehydes also proceeded with high enantioselectivity (**8r–8u**) following minor modifications of the reaction conditions (1,2-dichloroethane [DCE] as the solvent, 20 mol% MgPhPO₃ additive). In the case of asymmetric trisubstituted alkene **1e**, an inseparable mixture of **8v** and **8w** (itself a diastereomixture) was produced with moderate regioselectivity (regioisomeric ratio; rr = **8v**/**8w** = 1.9/1). Nevertheless, both the reactivity and enantioselectivity of **8v** were very high: use of 2.5 mol% and 0.5 mol% loadings of the chromium catalyst and photocatalyst **11**, respectively, led to the products in 97% combined yield, with **8v** in 96% ee. Major isomer **8v** presumably derives from prenylchromium species with the chromium atom at the terminal carbon, while minor isomer **8w** originates from 2-methyl but-2-enylchromium species with chromium at the terminal carbon. We anticipate that improving the regioselectivity so that the carbon-centered radical can be intercepted by the metal complex in the case of asymmetric alkenes will be a very important avenue for future research. In addition, linear terminal alkenes and disubstituted internal alkenes (e.g. 1-hexene and 2-butene) were unreactive under the current optimal conditions probably due to their high oxidation potentials.

The following experimental results provide key insights into the reaction mechanism (see ESI† for details). First, the addition of TEMPO (2,2,6,6-tetramethylpiperidin-1-oxyl) as a radical



Table 2 Substrate scope of catalytic asymmetric allylation^a

		yield (%) ee (%)		yield (%) ee (%)				
1	8	1	8	1	8			
 1a		8a: R = H	65 ^b	99		8l: R = H	86 ^c	88
		8b: R = <i>p</i> -Cl	82	99		8m: R = <i>o</i> -Me	50 ^d	96
		8c: R = <i>p</i> -Br	81	98		8n: R = <i>m</i> -Me	85 ^e	90
		8d: R = <i>p</i> -I	46	99		8o: R = <i>p</i> -Me	97 ^e	95
		8e: R = <i>m</i> -COMe	46	99		8p: R = <i>p</i> -MeO	39 ^d	96
		8f: R = <i>p</i> -CO ₂ Me	80	99				
		8g: R = <i>p</i> -CF ₃	63	99				
 1b		8h: R = H	59	99		8q	33 ^f	93
		8i: R = <i>p</i> -Cl	55	99				
 1c		8j: R = H	56 ^b	99		8r	90 ^g	99
		8k: R = <i>p</i> -Cl	47	99				
 1e		8v	97 ^c	96		8s	69 ^h	86
		8w				1.9/1 rr	8t	95 ^h
						8u	78 ^h	85

^a General reaction conditions: aldehyde **2** (0.25 mmol), alkene **1** (5.0 mmol), CrCl₂ (0.0125 mmol), L5 (0.0125 mmol), **10** (0.00625 mmol), and Mg(ClO₄)₂ (0.25 mmol) were reacted in DCM (2.5 mL) at room temperature under 430 nm LED irradiation for 12 h. Yield is isolated yield. The diastereomeric ratio was >20/1 in each case (**8a–8k**), as determined by ¹H NMR analysis of the crude mixture. The enantioselectivity was determined by chiral stationary HPLC analysis after isolation. ^b CrCl₂ (10 mol%) and L5 (10 mol%) were used. ^c Alkene (2 equiv.), CrCl₂ (2.5 mol%), L5 (2.5 mol%), **11** (0.5 mol%), Mg(ClO₄)₂ (1 equiv.), and DCM (0.125 M) were used. ^d Alkene (20 equiv.), CrCl₃·3THF (10 mol%), NaOt-Bu (30 mol%), L5 (10 mol%), **11** (1.25 mol%), Mg(ClO₄)₂ (1 equiv.), and DCM (0.0625 M) were used. ^e Alkene (5 equiv.), CrCl₂ (10 mol%), L5 (10 mol%), **11** (1.25 mol%), Mg(ClO₄)₂ (1 equiv.), and DCM (0.0625 M) were used. ^f Alkene (20 equiv.), CrCl₂ (20 mol%), L5 (20 mol%), **11** (5 mol%), Mg(ClO₄)₂ (1 equiv.), and DCM (0.0625 M) were used. ^g Alkene (5 equiv.), CrCl₂ (10 mol%), L5 (10 mol%), **11** (5 mol%), Mg(ClO₄)₂ (1 equiv.), and DCE (0.05 M) were used. ^h Alkene (20 equiv.), CrCl₂ (20 mol%), L5 (20 mol%), **11** (5 mol%), MgPhPO₃ (20 mol%), and DCE (0.1 M) were used. Reaction time was 48 h.

trapping agent to the reaction between **1a** and **2a** under otherwise optimized conditions completely inhibited the desired reaction. A TEMPO adduct of **1a** at the terminal carbon was detected by ¹H NMR analysis of the crude mixture after the workup. This result supports our hypothesis that the reaction proceeds through carbon-centered radicals derived from alkene **1**. Second, we performed a radical clock experiment using 2-phenylcyclopropylcarbaldehyde and **1d**. The reaction proceeded with 77% yield without any cyclopropane ring-opening, indicating that ketyl radicals derived from aldehydes are not involved in the catalytic cycle. These findings, together with the observation that the presence of the chromium complex was

essential for the reaction (Table 1, entry 1), are consistent with our working hypothesis for the reaction mechanism depicted in Fig. 2.

To clarify the electron-transfer dynamics between **1a** and the photoexcited **10**, we examined the transient absorption measurements as shown in Fig. 3(a). Laser flash irradiation ($\lambda = 355$ nm) of **10** gave the electron-transfer state (Acr⁻Xyl⁺). The spectrum furnished absorption peaks at $\lambda_{\text{max}} = 520$ nm (ref. 24) and 700 nm,²⁵ which attributed to the acridinyl radical moiety (Acr⁻) and the xylyl radical cation moiety (Xyl⁺), respectively (Fig. 3(a)). The time profiles of the decay at 700 nm due to the Xyl⁺ moiety obeyed pseudo-first-order kinetics. The decay rate





Fig. 3 Detection of radical intermediates in the photocatalytic redox cycle. (a) Transient absorption spectrum of **10** (50 μM) measured in DCM at 200 μs after laser excitation at 355 nm. (b) Relationship between the decay rate constant (k_{obs}) of the $\text{Xyl}^{\bullet+}$ moiety observed at 700 nm and the concentration of **1a**. (c) Time profiles at 520 nm of $\text{Acr}^{\bullet}-\text{Xyl}$ generated by photoexcitation of $\text{Acr}^{\bullet}-\text{Xyl}$ (50 μM) with cyclohexene (300 mM) in the absence (black) and presence (red) of $\text{Mg}(\text{ClO}_4)_2$.

constant (k_{obs}) linearly increased with the concentration of **1a** (Fig. 3(b)). The rate constant of electron transfer from **1a** to the acridinyl radical moiety of $\text{Acr}^{\bullet}-\text{Xyl}^{\bullet+}$ was determined from the linear plot to be $2.2 \times 10^5 \text{ M}^{-1} \text{ s}^{-1}$. Thus, electron transfer efficiently occurred to yield **3** and the reduced **10** ($\text{Acr}^{\bullet}-\text{Xyl}$) as the initial step of the photocatalytic redox process.

Furthermore, to confirm that the dramatically increased reactivity in the presence of additive $\text{Mg}(\text{ClO}_4)_2$ was due to the increased concentration of the radical pair (**3** and $\text{Acr}^{\bullet}-\text{Xyl}$) generated by electron transfer from **1a** to the electron-transfer state of **10** ($\text{Acr}^{\bullet}-\text{Xyl}^{\bullet+}$), we monitored the initial transient absorption intensities due to $\text{Acr}^{\bullet}-\text{Xyl}$ ($\lambda_{\text{max}} = 520 \text{ nm}$) generated by laser irradiation of **10** with a large excess of **1a** (300 mM) in the absence and presence of $\text{Mg}(\text{ClO}_4)_2$ (Fig. 3(c)). The initial intensity in the presence of $\text{Mg}(\text{ClO}_4)_2$ was 1.9 times higher than that in the absence of $\text{Mg}(\text{ClO}_4)_2$ (Fig. 3(c)). The radical pair is efficiently stabilized in the presence of $\text{Mg}(\text{ClO}_4)_2$ salt by the electrostatic interaction of **3** with ClO_4^- .²⁰ Therefore, the concentration of cation radical **3** is enhanced by the presence of $\text{Mg}(\text{ClO}_4)_2$, and this is likely the reason for the dramatically higher product yield in the presence of $\text{Mg}(\text{ClO}_4)_2$ (Table 1, entry 7 vs. 12).²⁶

Conclusions

In conclusion, we developed the first catalytic asymmetric allylation of aldehydes using unactivated hydrocarbon alkenes as pronucleophiles. The reaction enabled direct access to

enantiomerically and diastereomerically-enriched homoallylic alcohols, starting from readily available and stable substrates. Critical to the success of the reaction was the development of an asymmetric hybrid catalyst system comprising an acridinium photoredox catalyst and a chiral chromium complex catalyst. The hybrid catalysis enabled a key radical-polar crossover process involving the catalytic generation of chiral and nucleophilic (*i.e.*, polar) organometallic species from simple alkenes *via* allylic $\text{C}(\text{sp}^3)\text{-H}$ activation. Further studies to improve the efficiency of the process, fully elucidate the reaction mechanism, and expand the substrate scope are ongoing.

Conflicts of interest

There are no conflicts to declare.

Acknowledgements

This work was supported in part by JSPS KAKENHI Grant Numbers JP17H06442 (M. K.) (Hybrid Catalysis), 17H01522 (M. K.), 17K19479 (M. K.), 18H05969 (H. M.), 17H0310 (K. O.), 16K13964 (K. O.), and 18H04650 (K. O.) (Hybrid Catalysis). Authors deeply thanks to Prof. Shunichi Fukuzumi (Ewha Womans University, Korea) for the useful discussion and transient absorption measurements.

Notes and references

- For selected recent reviews on catalytic enantioselective $\text{C}(\text{sp}^3)\text{-H}$ bond functionalization, see: (a) R. Giri, B.-F. Shi, K. M. Engle, N. Maugele and J.-Q. Yu, *Chem. Soc. Rev.*, 2009, **38**, 3242; (b) Q. Lu and F. Glorius, *Angew. Chem., Int. Ed.*, 2017, **56**, 49; (c) T. G. Saint-Denis, R.-Y. Zhu, G. Chen, Q.-F. Wu and J.-Q. Yu, *Science*, 2018, **359**, eaa04798.
- For selected recent reviews on stereoselective allylation of carbonyl compounds, see: (a) P. V. Ramachandran, *Aldrichimica Acta*, 2002, **35**, 23; (b) S. E. Denmark and J. Fu, *Chem. Rev.*, 2003, **103**, 2763; (c) C.-M. Yu, J. Youn and H.-K. Jung, *Bull. Korean Chem. Soc.*, 2006, **27**, 463; (d) I. Marek and G. Sklute, *Chem. Commun.*, 2007, 1683; (e) D. G. Hall, *Synlett*, 2007, **11**, 1644; (f) G. C. Hargaden and P. J. Guiry, *Adv. Synth. Catal.*, 2007, **349**, 2407; (g) H. Yamamoto and M. Wadamoto, *Chem.-Asian J.*, 2007, **2**, 692; (h) H. Lachance and D. G. Hall, *Org. React.*, 2009, **73**, 1; (i) S. B. Han, I. S. Kim and M. J. Krische, *Chem. Commun.*, 2009, 7278; (j) M. Yus, J. C. González-Gómez and F. Foubelo, *Chem. Rev.*, 2011, **111**, 7774; (k) J. Moran and M. J. Krische, in *Asymmetric Synthesis: More Methods and Applications*, ed. M. Christmann and S. Bräse, Wiley-VCH, Weinheim, Germany, 2012, p. 187; (l) M. Yus, J. C. González-Gómez and F. Foubelo, *Chem. Rev.*, 2013, **113**, 5595; (m) H.-X. Huo, J. R. Duvall, M.-Y. Huang and R. Hong, *Org. Chem. Front.*, 2014, **1**, 303; (n) Q. Tian and G. Zhang, *Synthesis*, 2016, **48**, 4038; (o) P. Kumar, D. Tripathi, B. M. Sharma and N. Dwivedi, *Org. Biomol. Chem.*, 2017, **15**, 733; (p) S. W. Kim, W. Zhang and M. J. Krische, *Acc. Chem. Res.*, 2017, **50**, 2371; (q)



- P.-S. Wang, M.-L. Shen and L.-Z. Gong, *Synthesis*, 2018, **50**, 956; (r) D. M. Sedgwick, M. N. Grayson, S. Fustero and P. Barro, *Synthesis*, 2018, **50**, 1935; (s) K. Spielmann, G. Niel, R. M. de Figueiredo and J.-M. Campagne, *Chem. Soc. Rev.*, 2018, **47**, 1159; (t) M. Holmes, L. A. Schwartz and M. J. Krische, *Chem. Rev.*, 2018, **118**, 6026.
- 3 For selected reviews on catalytic asymmetric carbonyl ene reactions, see: (a) K. Mikami and M. Shimizu, *Chem. Rev.*, 1992, **92**, 1021; (b) D. J. Berrisford and C. Bolm, *Angew. Chem., Int. Ed.*, 1995, **34**, 1717; (c) *Comprehensive Asymmetric Catalysis*, ed. K. Mikami, M. Terada, E. N. Jacobsen, A. Pfaltz and H. Yamamoto, Springer, Berlin, Heidelberg, 1999, p. 1143; (d) L. C. Dias, *Curr. Org. Chem.*, 2000, **4**, 305; (e) K. Mikami and T. Nakai, in *Catalytic Asymmetric Synthesis*, ed. I. Ojima, Wiley-VCH, New York, 2000, p. 543; (f) M. L. Clarke and M. B. France, *Tetrahedron*, 2008, **64**, 9003.
- 4 Catalytic allylic C(sp³)-H activation reported so far mainly generates electrophilic π -allylmetal complexes. For selected reviews of allylic C(sp³)-H activation, see: (a) T. Jensen and P. Fristrup, *Chem.-Eur. J.*, 2009, **15**, 9632; (b) G. Liu and Y. Wu, *Top. Curr. Chem.*, 2010, **292**, 195; (c) C. J. Engelin and P. Fristrup, *Molecules*, 2011, **16**, 951; (d) C. Liu, H. Zhang, W. Shi and A. Lei, *Chem. Rev.*, 2011, **111**, 1780; (e) C. S. Yeung and V. M. Dong, *Chem. Rev.*, 2011, **111**, 1215; (f) B. J. Li and Z. J. Shi, *Chem. Soc. Rev.*, 2012, **41**, 5588; (g) F. Liron, J. Oble, M. M. Lorion and G. Poli, *Eur. J. Org. Chem.*, 2014, 5863; (h) C. Zheng and S. L. You, *RSC Adv.*, 2014, **4**, 6173; (i) C. G. Newton, S. G. Wang, C. C. Oliveira and N. Cramer, *Chem. Rev.*, 2017, **117**, 8908.
- 5 Z.-L. Tao, X.-H. Li, Z.-Y. Han and L.-Z. Gong, *J. Am. Chem. Soc.*, 2015, **137**, 4054.
- 6 T. Mita, S. Hanagata, K. Michigami and Y. Sato, *Org. Lett.*, 2017, **19**, 5876.
- 7 J. L. Schwarz, F. Schäfers, A. Tlahuext-Aca, L. Lückemeier and F. Glorius, *J. Am. Chem. Soc.*, 2018, **140**, 12705. The racemic variant exhibited broad substrate scope and excellent diastereoselectivity.
- 8 For chiral Brønsted base-catalyzed enantioselective allylation of ketones with special hydrocarbon alkenes (*i.e.*, skipped enynes), see: X.-F. Wei, X.-W. Xie, Y. Shimizu and M. Kanai, *J. Am. Chem. Soc.*, 2017, **139**, 4647.
- 9 For Brønsted base-catalyzed racemic allylation of imines with hydrocarbon alkenes, see: W. Bao, H. Kossen and U. Schneider, *J. Am. Chem. Soc.*, 2017, **139**, 4362.
- 10 For related methods for the generation of organonickel species, see: (a) C. L. Joe and A. G. Doyle, *Angew. Chem., Int. Ed.*, 2016, **55**, 4040; (b) D. T. Ahneman and A. G. Doyle, *Chem. Sci.*, 2016, **7**, 7002; (c) D. R. Heitz, J. C. Tellis and G. A. Molander, *J. Am. Chem. Soc.*, 2016, **138**, 12715; (d) B. J. Shields and A. G. Doyle, *J. Am. Chem. Soc.*, 2016, **138**, 12719; (e) M. H. Shaw, V. W. Shurtleff, J. A. Terrett, J. D. Cuthbertson and D. W. C. MacMillan, *Science*, 2016, **352**, 1304; (f) X. Zhang and D. W. C. MacMillan, *J. Am. Chem. Soc.*, 2017, **139**, 11353; (g) Y.-Y. Gui, L.-L. Liao, L. Sun, Z. Zhang, J.-H. Ye, G. Shen, Z.-P. Lu, W.-J. Zhou and D.-G. Yu, *Chem. Commun.*, 2017, **53**, 1192; (h) Y.-Y. Gui, X.-W. Chen, W.-J. Zhou and D.-G. Yu, *Synlett*, 2017, **28**, 2581; (i) C. Le, Y. Liang, R. W. Evans, X. Li and D. W. C. MacMillan, *Nature*, 2017, **547**, 79; (j) H.-P. Deng, X.-Z. Fan, Z.-H. Chen, Q.-H. Xu and J. Wu, *J. Am. Chem. Soc.*, 2017, **139**, 13579; (k) Y.-Y. Gui, Z.-X. Wang, W.-J. Zhou, L.-L. Liao, L. Song, Z.-B. Yin, J. Li and D.-G. Yu, *Asian J. Org. Chem.*, 2018, **7**, 537; (l) H. Fuse, M. Kojima, H. Mitsunuma and M. Kanai, *Org. Lett.*, 2018, **20**, 2042; (m) S. Y. Go, G. S. Lee and S. H. Hong, *Org. Lett.*, 2018, **20**, 4691; (n) J. Twilton, M. Christensen, D. A. DiRocco, R. T. Ruck, I. W. Davies and D. W. C. MacMillan, *Angew. Chem., Int. Ed.*, 2018, **57**, 5369; (o) L. Huang and M. Rueping, *Angew. Chem., Int. Ed.*, 2018, **57**, 10333; (p) I. B. Perry, T. W. Brewer, P. J. Sarver, D. M. Schlutz, D. A. DiRocco and D. W. C. MacMillan, *Nature*, 2018, **560**, 70; (q) Y. Shen, Y. Gu and R. Martin, *J. Am. Chem. Soc.*, 2018, **140**, 12200; (r) L. K. G. Ackerman, J. I. M. Alvarado and A. G. Doyle, *J. Am. Chem. Soc.*, 2018, **140**, 14059; (s) D.-M. Yan, C. Xiao and J.-R. Chen, *Chem*, 2018, **4**, 2496; (t) L. Zhang, X. Si, Y. Yang, M. Zimmer, S. Witzel, K. Sekine, M. Rudolph and A. S. K. Hashmi, *Angew. Chem., Int. Ed.*, 2018, **57**, DOI: 10.1002/anie.201810526.
- 11 For related methods for the generation of organopalladium species, see: (a) S. Kato, Y. Saga, M. Kojima, H. Fuse, S. Matsunaga, A. Fukatsu, M. Kondo, S. Masaoka and M. Kanai, *J. Am. Chem. Soc.*, 2017, **139**, 2204; (b) U. K. Sharma, H. P. L. Gemoets, F. Schröder, T. Noël and E. V. Van der Eycken, *ACS Catal.*, 2017, **7**, 3818.
- 12 For a related method for the generation of organocobalt species, see: S. M. Thullen and T. Rovis, *J. Am. Chem. Soc.*, 2017, **139**, 15504.
- 13 For the generation of chiral organometallic species through homolytic cleavage of a stable C(sp³)-H bond and subsequent oxidative trap by a chiral metal complex, which was applied to a catalytic asymmetric coupling reaction (oxidative benzylic C(sp³)-H cyanation), see: W. Zhang, F. Wang, S. D. McCann, D. Wang, P. Chen, S. S. Stahl and G. Liu, *Science*, 2016, **353**, 1014. One preliminary example (54% ee) with this reaction pattern was also described in ref. 10q.
- 14 R. Zhou, H. Liu, H. Tao, X. Yu and J. Wu, *Chem. Sci.*, 2017, **8**, 4654.
- 15 For a discussion of the feasibility of the working hypothesis shown in Fig. 2 based on the redox potential of each intermediate, see ESI.†
- 16 T. Tsudaka, H. Kotani, K. Ohkubo, T. Nakagawa, N. V. Tkachenko, H. Lemmetyinen and S. Fukuzumi, *Chem.-Eur. J.*, 2017, **23**, 1306.
- 17 For selected examples of catalytic asymmetric Nozaki-Hiyama-Kishi allylation reaction, see: (a) M. Bandini, P. G. Cozzi, P. Melchiorre and A. Umani-Ronchi, *Angew. Chem., Int. Ed.*, 1999, **38**, 3357; (b) A. Berkessel, D. Menche, C. A. Sklorz, M. Schröder and I. Paterson, *Angew. Chem., Int. Ed.*, 2003, **42**, 1032; (c) M. Inoue, T. Suzuki and M. Nakada, *J. Am. Chem. Soc.*, 2003, **125**, 1140; (d) M. Kurosu, M.-H. Lin and Y. Kishi, *J. Am. Chem. Soc.*, 2004, **126**, 12248; (e) J.-Y. Lee, J. J. Miller, S. S. Hamilton and



- M. S. Sigman, *Org. Lett.*, 2005, **7**, 1837; (f) G. Xia and H. Yamamoto, *J. Am. Chem. Soc.*, 2006, **128**, 2554; (g) J. J. Miller and M. S. Sigman, *J. Am. Chem. Soc.*, 2007, **129**, 2752; (h) Z. Zhang, J. Huang, B. Ma and Y. Kishi, *Org. Lett.*, 2008, **10**, 3073; (i) Q.-H. Deng, H. Wadepohl and L. H. Gade, *Chem.-Eur. J.*, 2011, **17**, 14922.
- 18 C. Chen, K. Tagami and Y. Kishi, *J. Org. Chem.*, 1995, **60**, 5386.
- 19 G. Desimoni, G. Faita and K. A. Jørgensen, *Chem. Rev.*, 2006, **106**, 3561.
- 20 (a) P. A. Thompson and J. D. Simon, *J. Am. Chem. Soc.*, 1993, **115**, 5657; (b) T. M. Bockman, S. M. Hubig and J. K. Kochi, *J. Am. Chem. Soc.*, 1998, **120**, 2826; (c) T. Yabe and J. K. Kochi, *J. Am. Chem. Soc.*, 1992, **114**, 4491; (d) V. N. Grosso, C. M. Previtali and C. A. Chesta, *Photochem. Photobiol.*, 1998, **68**, 481; (e) R. A. Marcus, *J. Phys. Chem. B*, 1998, **102**, 10071; (f) T. Kluge and H. Knoll, *J. Photochem. Photobiol., A*, 2000, **130**, 95; (g) E. V. Vakarin, M. F. Holovko and P. Piotrowiak, *Chem. Phys. Lett.*, 2002, **363**, 7; (h) K. Okamoto, K. Ohkubo, K. M. Kadish and S. Fukuzumi, *J. Phys. Chem. A*, 2004, **108**, 10405.
- 21 K. N. Mahendra and R. C. Mehrotra, *Synth. React. Inorg. Met.-Org. Chem.*, 1990, **20**, 963.
- 22 K. Sugimoto, S. Aoyagi and C. Kibayashi, *J. Org. Chem.*, 1997, **62**, 2322.
- 23 In the reaction of *p*-methoxy benzaldehyde and **1d**, NMR yields of **8p** were 33% and 62% by using CrCl₂ and CrCl₃·3THF–NaOt-Bu catalysts, respectively.
- 24 S. Fukuzumi, H. Kotani, K. Ohkubo, S. Ogo, N. V. Tkachenko and H. Lemmetyinen, *J. Am. Chem. Soc.*, 2004, **126**, 1600.
- 25 K. Ohkubo, K. Suga, K. Morikawa and S. Fukuzumi, *J. Am. Chem. Soc.*, 2003, **125**, 12850.
- 26 On the other hand, the role of Mg(ClO₄)₂ (or perchlorate in general, see Table 1, entry 7 vs. 9–12) in enhancing the enantioselectivity is still unclear. We assume that chiral ligand **L5** remains coordinated to the chromium atom during the reaction in the presence of stoichiometric Mg(ClO₄)₂; the reaction between **1a** and **2a** did not proceed at all by premixing of **L5** with Mg(ClO₄)₂. See ESI† for details.

